Available online at www.sciencedirect.com
SCIENCE DIRECT®
Journal of Solid State Chemistry 177 (2004) 1933–1938
JOURNAL OF SOLID STATE CHEMISTRY
http://elsevier.com/locate/jssc

Phase equilibrium in the system Y–Fe–O at 1100°C

Kenzo Kitayama,* Masanori Sakaguchi, Youhei Takahara, Hiroyuki Endo, and Hirofumi Ueki

Department of Applied Chemistry and Biotechnology, Faculty of Engineering, Niigata Institute of Technology, Kashiwazaki, Niigata 945-1195, Japan

Received 8 August 2003; received in revised form 12 December 2003; accepted 18 December 2003

Abstract

Phase equilibrium was established in the Y–Fe–O system at 1100°C by varying the oxygen partial pressure from $-\log(P_{O_2}/\text{atm}) = 15.00$ to 0, allowing construction of a phase diagram at 1100°C for the system Y_2O_3–Fe–Fe_2O_3. In the system, two ternary compounds, $YFeO_3$ and $Y_3Fe_5O_{12}$, were stable and had nonstoichiometric composition, whereas YFe_2O_4 was not found to be stable. The present result was different from that of previous studies at 1200°C, in which YFe_2O_4 was stable, along with the above two ternary compounds. Lattice constants of $YFeO_3$ and $Y_3Fe_5O_{12}$, prepared in air by a quenching method, were determined and compared with previous values, and showed close agreement. The standard Gibbs energy changes of the reactions in the Fe–O system, $Fe + 1/2O_2 = FeO$, $3FeO + 1/2O_2 = Fe_3O_4$, and $2/3Fe_3O_4 + 1/6O_2 = Fe_2O_3$, were determined, and the obtained values were compared with the previous values. The standard Gibbs energy changes of the reactions, $Fe + 1/2Y_2O_3 + 3/4O_2 = YFeO_3$, and $3YFeO_3 + 2/3Fe_3O_4 + 1/6O_2 = Y_3Fe_5O_{12}$, were calculated from the oxygen partial pressures in equilibrium.

Keywords: Phase equilibrium; Thermogravimetry; Yttrium-iron oxide; Gibbs energy

1. Introduction

Phase relations in the Fe–O system have been reported from the standpoint of steelmaking [1,2,3]. As is well known, the Fe–O system includes three oxides, "FeO", Fe_3O_4, and Fe_2O_3. "FeO" has a cubic structure and forms a metal defect solid solution. Fe_3O_4 has an inverse spinel structure and a low solid solution range in the oxygen-rich side, and the solid solution range changes with temperature. Fe_2O_3 has a stoichiometric composition and rhombohedral crystal system.

The oxygen partial pressure in equilibrium with Fe and FeO, with FeO and Fe_3O_4, and with Fe_3O_4 and Fe_2O_3 were obtained from JANAF data [4] to be 13.33, 11.75, and 3.74 in $-\log(P_{O_2}/\text{atm})$ at 1100°C, respectively.

The phases in the Y–Fe–O system are of important technological interest, particularly in view of physical properties. As is well known, in the Y–Fe–O system, $YFeO_3$ and $Y_3Fe_5O_{12}$(YIG) are stable as ternary compounds. Recently Kimizuka and Katsura [5] have found a new phase, YFe_2O_4, that is stable at 1200°C, and it has a hexagonal crystal system with $a = 6.090$ Å and $c = 24.788$ Å. Piekarczyk et al. [6] have reported YFe_2O_4 phase to be stable above 1010°C. According to Kato et al. [7], the crystal structure of this compound is a new type for AB_2X_4, where A and B are cations and X is an anion, and belongs to the trigonal system with the space group $R3/m$. The structure consists of alternate layers of Ln_2O_3 and Fe_4O_5, and thus the anisotropies both in the magnetic exchange interaction and the electrical conductivity are expected.

The crystal structure and magnetic properties of YFe_2O_4, together with $ErFe_2O_4$, have been studied by Matsumoto et al. [8], and the pressure dependence of the magnetic phase transitions of YFe_2O_4 was found.

The EMF measurememt by a solid electrolyte galvanic cell on the reaction, $Fe + 3/2NiO + 1/2Y_2O_3 = 3/2Ni + YFeO_3$, was performed at 1200–1400 K, and in combination with Gibbs energy of formation of NiO from Charette et al. [9], Gibbs energy of the reaction, $Fe + 1/2Y_2O_3 + 3/4O_2 = YFeO_3$, was calculated [10].

*Corresponding author. Fax: +81-025-722-8142.
E-mail address: kitayama@acb.niit.ac.jp (K. Kitayama).

0022-4596/$ - see front matter © 2004 Elsevier Inc. All rights reserved.
doi:10.1016/j.jssc.2003.12.040

The objectives of the present study are to: (1) establish a detailed phase diagram of Y–Fe–O system at 1100°C as a function of oxygen partial pressure; (2) ascertain whether or not the phase diagram at 1100°C is different from that at 1200°C; (3) determine thermochemical properties based on the phase diagram at 1100°C.

2. Experimental

Analytical grade Y_2O_3 (99.9%) and Fe_2O_3 (99.9%) were used as starting materials.

Both the oxides were calcined at 1100°C. Mixtures having desired ratios of Y_2O_3/Fe_2O_3 were prepared by mixing thoroughly in an agate mortar and performing repeated calcination during the intermediate mixing. This was followed by the same procedures described previously [11]. The thermogravimetric method was used in the present experiment; oxygen partial pressure was varied by passing a gas or mixed gases through the furnace.

The desired oxygen partial pressures were obtained by use of mixed gases of CO_2 and H_2 and of CO_2 and O_2, and single-component gases of O_2 and CO_2. The apparatus and procedures for controlling the oxygen partial pressure and maintaining a constant temperature, the method of thermogravimetry, and the criterion for the establishment of equilibrium were the same as described in the previous paper [11]. The method of establishing equilibrium can be briefly described as follows. To ensure equilibrium, the equilibrium weight of each sample at a particular oxygen partial pressure was determined from both sides of the reaction; that is, as the oxygen partial pressure was increased from a low value and as it was decreased from a high value. The balance, furnace, and gas mixer are schematically shown in Ref. [12]. The furnace was installed vertically, and a mullite tube wound with Pt 60%–Rh 40% alloy wire served as its heating element. Mixed gases, which ensure the desired oxygen partial pressures, passed from the bottom of the furnace to the top.

The identification of phases and the determination of lattice constants were performed by use of a Rint 2500 Rigaku X-ray diffractometer, employing Ni-filtered Cu$K\alpha$ radiation. An external standard silicon was used to calibrate 2θ.

3. Results and discussions

3.1. Phase equilibrium

3.1.1. Fe–O system

As described above, the Fe–O system contains three oxides, FeO, Fe_3O_4, and Fe_2O_3. In the present experiment, Fe–O system was reinvestigated by use of the present apparatus and techniques. The results are as follows. Fig. 1(a) shows the oxygen partial pressure, $-\log(P_{O_2}/\text{atm})$, versus the weight changes, $W_{O_2}W_T$ of the Fe–O system. Here, W_{O_2} is the weight increase of a sample from the reference weight at $\log(P_{O_2}/\text{atm}) = -15.00$, at which Fe is stable, and W_T is the total weight gained from reference state to the state at 1 atm O_2. As is evident from Fig. 1(a), weight breaks are found at 13.25, 10.86, and 3.20 in $-\log(P_{O_2}/\text{atm})$. These values correspond to the equilibrium oxygen partial pressure of the three reactions: (1) $Fe + 1/2O_2 = FeO$, (2) $3FeO + 1/2O_2 = Fe_3O_4$, and (3) $2/3Fe_3O_4 + 1/6O_2 = Fe_2O_3$, listed in Table 4.

As is well known, the phase FeO has a nonstoichiometric composition. Fig. 1(b) shows the relationship between the oxygen partial pressure and the composition, O/Fe mole ratio, of the Fe–O system. From this figure, the so-called wustite solid solution is stable from $-\log(P_{O_2}/\text{atm}) = 13.25$ to 10.86 (from A to B in Fig. 1(b)), and the $-\log(P_{O_2}/\text{atm})$ vs. the O/Fe mole ratio of FeO solid solution is represented by a linear equation: $N_O/N_{Fe} = 4.077 \times 10^{-2} \log P_{O_2} + 1.577$. Here, N_O and N_{Fe} represent the mole fraction of oxygen and Fe in the

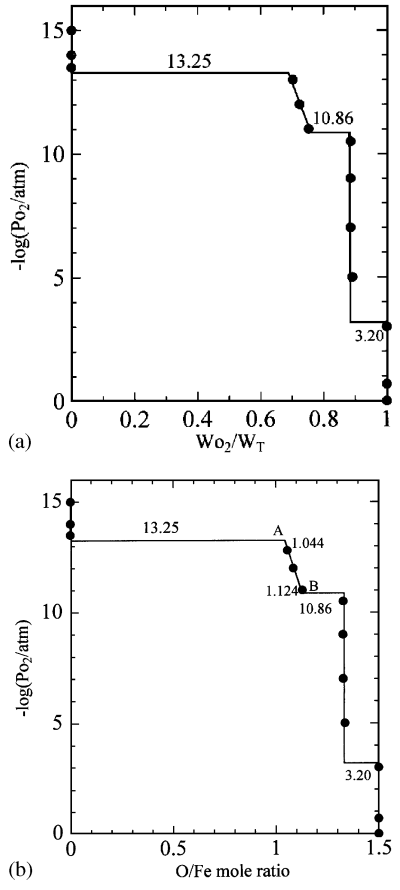

Fig. 1. (a) Relationship between the oxygen partial pressure, $\log(PO_2/\text{atm})$ and the weight change of samples, $W_{O_2}W_T$ in the Fe–O system, (b) Relationship between the oxygen partial pressure, $\log(P_{O_2}/\text{atm})$, and the O/Fe molar ratio in the Fe–O system.

FeO solid solution. This equation will be used to obtain the activity of Fe and FeO components in the solid solution by the Gibbs–Duem equation and can be solved to show that FeO phase would have an O/Fe mole ratio $=1.044$ at -13.25 and an O/Fe mole ratio $=1.124$ at -10.86 in $\log(P_{O_2}/\text{atm})$. As is well known, the stoichiometric FeO is not stable, and at the end composition of wustite, O/Fe mole ratio of 1.044 is in equilibrium with Fe metal at $-\log P_{O_2}=13.25$ and O/Fe mole ratio of 1.124 is in equilibrium with Fe_3O_4 at $-\log(P_{O_2}/\text{atm})=10.86$.

In Fe_3O_4, a slight weight increase has been observed from $-\log(P_{O_2}/\text{atm})=10.86$ to 3.20 as is well known, although it is not evident in Figs. 1(a) and (b), because of the scale of abscissa.

3.1.2. Y_2O_3–Fe–Fe_2O_3 system

Four samples having Y_2O_3/Fe_2O_3 mole ratios of 0.6/0.4, 0.4/0.6, 0.3/0.7, and 0.2/0.8 were prepared for thermogravimetry. Fig. 2 shows the oxygen partial pressure, $-\log(P_{O_2}/\text{atm})$, versus the weight changes, $W_{O_2}W_T$, for three representative samples: 0.6/0.4 (Fig. 2(a)), 0.4/0.6 (Fig. 2(b)), and 0.2/0.8 (Fig. 2(c)). Here, also, W_{O_2} is the weight increase of a sample from the reference weight at $\log(P_{O_2}/\text{atm})=-15.00$, at which Y_2O_3 and Fe are stable, and W_T is the total weight-gain from reference state to the state at 1 atm O_2, at which Y_2O_3 and $YFeO_3$, $YFeO_3$ and $Y_3Fe_5O_{12}$, and $Y_3Fe_5O_{12}$ and Fe_2O_3 were stable depending upon the total compositions of samples, as shown in Fig. 3. These phases were ascertained by an identification of phase. As evident from Fig. 2, weight breaks were found at 13.32, 13.25, 10.86, 6.88, and 3.20 in $-\log(P_{O_2}/\text{atm})$. These values correspond to the oxygen partial pressure in equilibrium with the three solid phases, $Y_2O_3+YFeO_3+Fe$, $YFeO_3+FeO+Fe$, $YFeO_3+FeO+Fe_3O_4$, $Fe_3O_4+YFeO_3+Y_3Fe_5O_{12}$, and $Y_3Fe_5O_{12}+Fe_3O_4+Fe_2O_3$, respectively.

Table 1 shows the identified phases in the Y–Fe–O system, along with the experimental conditions. Samples of about 500 mg were prepared for the identification of phases by means of the quenching method. Seven phases, Y_2O_3, Fe, FeO, Fe_3O_4, Fe_2O_3, $Y_3Fe_5O_{12}$, and $YFeO_3$, were evaluated by the powdered X-ray analysis

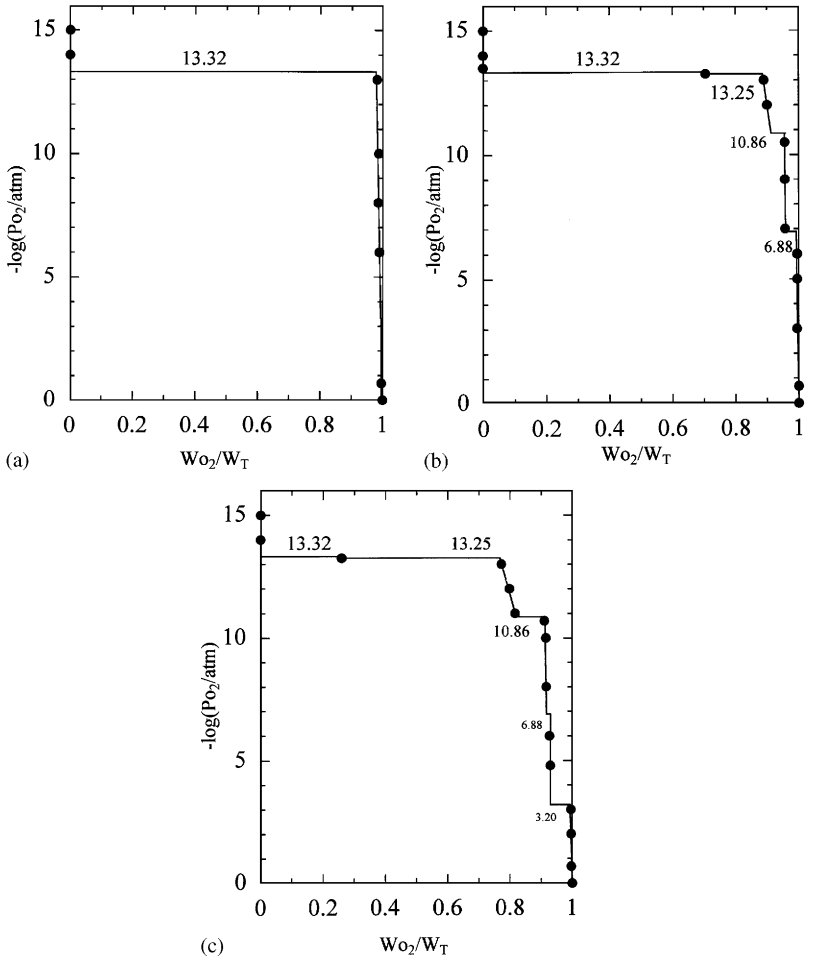

Fig. 2. Relationship between the oxygen partial pressure, $\log(P_{O_2}/\text{atm})$, and the weight change of the samples, $W_{O_2}W_T$. (a) $Y_2O_3/Fe_2O_3=0.6/0.4$, (b) $Y_2O_3/Fe_2O_3=0.4/0.6$, and (c) $Y_2O_3/Fe_2O_3=0.2/0.8$.

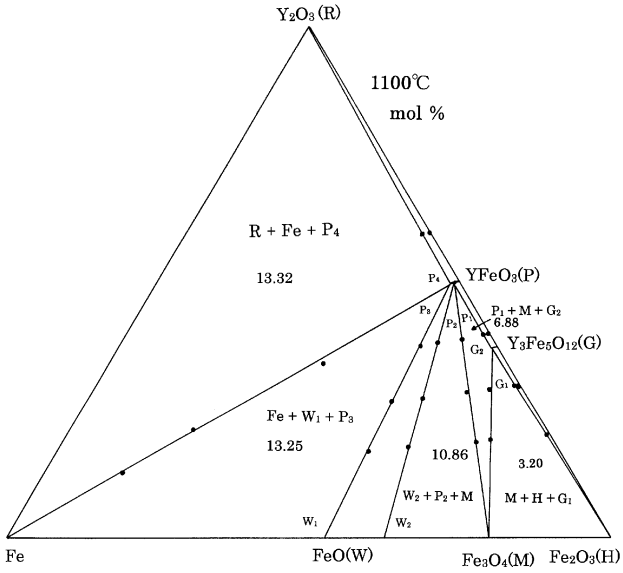

Fig. 3. Phase equilibrium in the Y_2O_3–Fe–Fe_2O_3 system at 1100°C. Numerical values indicated in the three phase regions are the oxygen partial pressures in $-\log(P_{O_2}/\text{atm})$ in equilibrium with solid phases shown in each region. Abbreviations are the same as those in Table 2.

Table 1
Identification of phases

Y_2O_3 (mol ratio)	Fe_2O_3 (mol ratio)	$-\log P_{O_2}$ (atm)	Time (h)	Phases
0	1.0	14.00	8.0	Fe
		13.00	8.0	FeO
		10.50	14.8	Fe_3O_4
		0.68	15.0	Fe_2O_3
0.2	0.8	14.00	7.0	Fe + Y_2O_3
		13.28	27.0	Fe + $YFeO_3$
		11.00	9.0	FeO + $YFeO_3$
		10.50	17.0	Fe_3O_4 + $YFeO_3$
		5.00	64.0	Fe_3O_4 + $Y_3Fe_5O_{12}$
		0.68	124.0	Fe_2O_3 + $Y_3Fe_5O_{12}$
0.3	0.7	14.00	7.0	Fe + Y_2O_3
		13.28	27.0	Fe + $YFeO_3$
		11.00	9.0	FeO + $YFeO_3$
		10.50	17.0	Fe_3O_4 + $YFeO_3$
		5.00	64.0	Fe_3O_4 + $Y_3Fe_5O_{12}$
		0.68	63.0	Fe_2O_3 + $Y_3Fe_5O_{12}$
0.4	0.6	14.00	7.0	Fe + Y_2O_3
		11.00	9.0	FeO + $YFeO_3$
		10.50	17.0	Fe_3O_4 + $YFeO_3$
		5.00	64.0	$YFeO_3$ + $Y_3Fe_5O_{12}$
		4.00	13.6	$YFeO_3$ + $Y_3Fe_5O_{12}$
		0.68	124.0	$YFeO_3$ + $Y_3Fe_5O_{12}$
0.6	0.4	14.00	7.0	Fe + Y_2O_3
		13.28	27.0	$YFeO_3$ + Y_2O_3
		10.50	17.0	$YFeO_3$ + Y_2O_3
		0.68	63.0	$YFeO_3$ + Y_2O_3

and were found to be stable under the experimental conditions. From the above results of thermogravimetry and the identification of the phase, a phase diagram was constructed for the Y_2O_3–Fe–Fe_2O_3 system, as shown in Fig. 3. The numerical values in the three solid fields in Fig. 3 are the values of $-\log P_{O_2}$ in equilibrium with the three solid phases, as described above. The nonstoichiometries of $YFeO_3$ and $Y_3Fe_5O_{12}$ were found, although both composition ranges were small.

As has already been reported [1–3], the Fe_3O_4 phase has a small nonstoichiometry, although this is not explicitly shown in Fig. 3, because of the figure's scale. Piekarczyk et al. [13] reported that "the phase diagram analysis shows for the entire temperature range investigated, from 900°C to 1250°C, that the garnet $Y_3Fe_5O_{12}$ can coexist with Fe_3O_4 and Fe_2O_3". In the present Fig. 3, the $Y_3Fe_5O_{12}$ can coexist with Fe_2O_3, Fe_3O_4, and $YFeO_3$.

The YFe_2O_4 phase, which Kimizuka et al. [5] found to be stable at 1200°C, was not stable at 1100°C. Piekarczyk et al. [6] also reported that the YFe_2O_4 phase is stable above 1010°C. The instability of the YFe_2O_4 phase is a striking difference from the previous reports. Below 1010°C, the present phase diagram is similar to that of Piekarcyk et al. [6].

$YFeO_3$ and $Y_3Fe_5O_{12}$ exhibit a slightly nonstoichiometric composition in the range of $\log(P_{O_2}/\text{atm}) = -13.32$ to 0 and the range of $\log(P_{O_2}/\text{atm}) = -6.68$ to 0, respectively. The relationship between the oxygen partial pressure and the composition of the $YFeO_3$ solid solution could be represented by an equation, $N_O/N_{YFeO_3} = 2.260 \times 10^{-3}(\log P_{O_2}) - 2.123 \times 10^{-3}$, obtained by the least-squares method. Here, N_O and N_{YFeO_3} represent the mole fraction of oxygen and $YFeO_3$ in the solid solution. This equation can be solved to show that yttrium–iron perovskite would be stoichiometric at 0 and $YFeO_{2.97}$ at −13.32 in terms of $\log(P_{O_2}/\text{atm})$, respectively.

Compositions, symbols, stability ranges in oxygen partial pressures of compounds and activities of components in the solid solutions are tabulated in Table 2. In the next section, these activities will be used in calculations of Gibbs energy change of reactions.

Table 2
Compositions, symbols, stability, ranges of oxygen partial pressures, and activities of components in solid solutions

Component	Compositions	Symbols	$-\log(P_{O_2}/\text{atm})$	$\log a_i$
FeO	$FeO_{1.027}$	W_1	13.25	0
	$FeO_{1.109}$	W_2	10.86	−0.102
$YFeO_3$	$YFeO_{2.98}$	P_1	6.88	0.0803
	$YFeO_{2.97}$	P_2	10.86	0.0310
	$YFeO_{2.97}$	P_3	13.25	~0
	$YFeO_{2.97}$	P_4	13.32	0
$Y_3Fe_5O_{12}$	$Y_3Fe_5O_{11.99}$	G_1	3.20	~0
	$Y_3Fe_5O_{11.99}$	G_2	6.88	0

Table 3
Lattice constants of $Y_3Fe_5O_{12}$ and $YFeO_3$

Sample		$-\log P_{O_2}$(atm)	Time (h)	Coexisting phase	a (A)	b (A)	c (A)	V (A^3)
$Y_3Fe_5O_{12}$								
Y_2O_3	Fe_2O_3							
0.4	0.6	0.68	124	$YFeO_3$	12.381(3)			1898.1(5)
0.2	0.8	0.68	124	Fe_2O_3	12.371(4)			1893.2(6)
Ref. [16]					12.380			
$YFeO_3$								
Y_2O_3	Fe_2O_3							
0.6	0.4	0.68	124	Y_2O_3	5.592(4)	7.601(5)	5.281(4)	224.5(3)
Ref. [17]					5.5946	7.6053	5.2817	

The lattice constants and the unit cell volume of $YFeO_3$ perovskite and $Y_3Fe_5O_{12}$ which were prepared in air were determined. The results are tabulated in Table 3, together with the previously reported values. Slight differences were found in the lattice constants.

3.2. Standard Gibbs energy change of reaction

On the basis of the established phase diagram, the standard Gibbs energy changes of reactions were determined by the equation, $\Delta G^0 = -RT\ln K$. Here, R is the gas constant, T absolute temperature, and K the equilibrium constant of the reaction.

As represented in Table 4, five chemical reactions are found in the established phase diagram. In calculation of the Gibbs energies of reactions the activity of each component in the solid solution has to be used. For example, as is apparent from the phase equilibrium, the activity of FeO in the reaction (1) is different from that of reaction (2). The activity of FeO component at the composition A in Fig. 1(b) that is in equilibrium with Fe should be different from that of FeO component at the composition B that is in equilibrium with Fe_3O_4. The Gibbs-Duhem equation was used to calculate the activities of Fe and FeO components in the FeO solid solution from the obtained N_O/N_{Fe} relation and the details of the calculation can be found in the report of Darken and Gurry [1] and in the book of Wagner [14].

The ΔG^0 value of $-174.2\,\mathrm{kJ\,mol^{-1}}$ for reaction (1) determined in the present investigation agrees well with the values -175.3 and $-175.6\,\mathrm{kJ\,mol^{-1}}$ calculated from JANAF Table 4 and Robie et al. [15]. For reaction (2), the present value of the oxygen partial pressure in equilibrium is identical to that of Darken and Gurry [1] that was published in 1945. The present ΔG^0 value for reaction (4) is in fairly good agreement with previous ones. Assuming that the activity of $YFeO_3$ component is unity, the present calculated ΔG^0 value for reaction (5) is comparable to that calculated from the equation, $\Delta G^0 = -84.1 + 0.0387\,T\,\mathrm{kJ\,mol^{-1}}$ $(1173 < T[\mathrm{K}] < 1523)$, of Piekarczyk et al. [6].

Table 4
Standard Gibbs energy changes of reactions

Reaction	$-\log(P_{O_2}/\mathrm{atm})$	$-\Delta G^0$/ kJ mol^{-1}
(1) $Fe + 1/2O_2 = FeO$	13.25	174.2
	13.33[b]	175.3[(4)]
	13.36[b]	175.6[(15)]
	13.30[(1)]	
(2) $3FeO + 1/2O_2 = Fe_3O_4$	10.86	150.8
	10.86	142.8[a]
	11.75[b]	154.6[(4)]
	11.46[b]	150.6[(15)]
	10.83[(1)]	
(3) $2/3Fe_3O_4 + 1/6O_2 = Fe_2O_3$	3.20	14.0
	3.74[b]	16.4[(4)]
	3.87[b]	17.0[(15)]
(4) $Fe + 1/2Y_2O_3 + 3/4O_2 = YFeO_3$	13.32	262.6
		263.4[(10)]
		258.7[c]
		258.7[(6)]
(5) $3YFeO_3 + 2/3Fe_3O_4 + 1/6O_2 = Y_3Fe_5O_{12}$	6.88	23.8
	6.88	30.1[d]
		31.0[(6)]

[a] Value calculated under the assumption that activity of FeO is unity.
[b] Values calculated from ΔG^0 values.
[c] Value calculated by combination with the data of Yamauchi (Ref. [10]) and data of the formation of NiO in Geological Survey Bulletin, 1452 (Ref. [15]).
[d] Activity of the $YFeO_3$ component is assumed to be unity.

4. Conclusion

1. Phase equilibrium in the system Y–Fe–O at 1100°C was established under an oxygen partial pressure from 0 to −15.00 in log(PO_2/atm).
2. Under the present experimental conditions, Y_2O_3, Fe, FeO, Fe_3O_4, Fe_2O_3, $YFeO_3$, and $Y_3Fe_5O_{12}$ phases are stable, whereas YFe_2O_4 is not stable. This is in striking contrast to the previous result at 1200°C.
3. Fe_3O_4, $YFeO_3$, and $Y_3Fe_5O_{12}$ were nonstoichiometric, but the range of the nonstoichiometry of Fe_3O_4 was too small to show in Figs. 1(a), (b) and 3.
4. Lattice constants of $YFeO_3$ and $Y_3Fe_5O_{12}$ were determined and were fairly in good agreement with previous values.

5. Standard Gibbs energies of reactions found in the phase diagram were calculated with the oxygen partial pressures in equilibrium with three solid phases.

References

[1] L.S. Darken, R.W. Gurry, J. Am. Chem. Soc. 67 (1945) 1398.
[2] L.S. Darken, R.W. Gurry, J. Am. Chem. Soc. 68 (1946) 798.
[3] A. Muan, E.F. Osborn, Phase Equilibria Among Oxides in Steelmaking, Addison-Wesley Publishing Company, Inc., Reading, MA, 1965.
[4] JANAF, Thermochemical Tables, 2nd Edition, NSRDS-NBS 37, 1971.
[5] N. Kimizuka, T. Katsura, J. Solid State Chem. 13 (1975) 176.
[6] W. Piekarczyk, W. Wepper, A. Rabenau, Z. Naturforsch. 34A (1979) 430.
[7] K. Kato, I. Kawada, N. Kimizuka, T. Katsura, Z. Kristallogr. 141 (1975) 314.
[8] T. Matsumoto, N. Mori, J. Iida, M. Tanaka, K. Siratori, F. Izumi, H. Asano, Physica B 180&181 (1992) 603.
[9] G.G. Charette, S.N. Flengas, J. Electrochem. Soc. 115 (1968) 796.
[10] S. Yamauchi, K. Fueki, T. Mukaibo, C. Nakayama, Bull. Chem. Soc. Jpn. 48 (1975) 1039.
[11] K. Kitayama, K. Nojiri, T. Sugihara, T. Katsura, J. Solid State Chem. 56 (1985) 1.
[12] K. Kitayama, J. Solid State Chem. 137 (1998) 255.
[13] W. Piekarczyk, W. Weppner, A. Rabenau, Mater. Sci. Monogr. 10 (1982) 679.
[14] C. Wagner, Thermodynamics of Alloys, Addison-Wesley Publishing Company Inc., Reading, MA, 1952.
[15] R.A. Robie, R.S. Hemingway, J.R. Fisher, Thermodynamic Properties of Minerals and Related Substances at 298.15 K and 1 Bar (10^5 Pascals) Pressure and at Higher Temperatures, Geological Survey Bulletin 1452, United States Goverment Printing Office, Washington, 1978.
[16] JCPDS, Card No. 43–0507.
[17] JCPDS, Card No. 39–1489.